Highlights on Spanish Astrophysics IX, Proceedings of the XII Scientific Meeting of the Spanish Astronomical Society held on July 18 – 22, 2016, in Bilbao, Spain. S. Arribas, A. Alonso-Herrero, F. Figueras, C. Hernández-Monteagudo, A. Sánchez-Lavega, S. Pérez-Hoyos (eds.)

On the chemical composition of the Milky Way outermost disc

A. Fernández-Martín[1], J.M. Vílchez[1], E. Pérez-Montero[1], and A. Mampaso[2]

[1] Instituto de Astrofísica de Andalucía (IAA-CSIC), 18008 Granada, Spain
[2] Instituto de Astrofísica de Canarias (IAC), 38200 La Laguna, Tenerife, Spain

Abstract

The knowledge of the chemical distribution towards the Galactic anticentre is a powerful method for understanding the history of formation and evolution of the Milky Way. In this contribution it is described the self-consistent study of the physical and chemical properties of a sample of 23 H II regions observed in the optical range and located in a range of Galactocentric distances from 11 kpc to 18 kpc. Chemical abundances were derived for all the regions and their distribution along the Galactocentric distances were fitted to obtain the radial gradients of O/H, N/H, N/O, S/H, Ar/H, and He/H across the outermost part of the MW. The distribution of elements heavier than helium shows a clear decrease with distance. Although a shallower slope at large Galactocentric distances is suggested by our data, it does not necessarily imply a flattening of the gradient in the outer disc, but clearly shows that a linear extrapolation of the inner slope is inconsistent with the observations.

1 Introduction

The chemical composition of the interstellar medium varies between galaxies and is both position and time dependent within a galaxy. A knowledge of the radial variations of metallicity across the galactic disc is central to our understanding of a wide variety of observed phenomena. The existence of a large-scale gradient in the Milky Way (MW) with H II regions was established by the pioneering work of [9], who found a decrease of metallicity with Galactic distances. Subsequently, several studies with H II regions have been carried out, firmly establishing the existence of a negative gradient of abundance of the elements heavier than helium in the disc of the MW. Nonetheless, the sampling of the whole Galactic disc is still poor and relatively few H II regions have been studied towards the Galactic anticentre region. This is also a handicap for the MW studies, compared with those for nearby external galaxies, and limits the application of models of galactic evolution.

2 Sample of HII regions

Resorting to the catalogues of [2], [5], and [7] we built the mother sample which includes 89 anticentre H II regions with $R_G > 11$ kpc observable from the northern hemisphere.

The observations were carried out in December 2009 and July 2010 using the ISIS double-armed spectrograph at the 4.2 m William Herschel Telescope covering the effective spectral range from 3200 Å to 10000 Å. Nine H II regions located at 11 kpc $<R_G<17$ kpc were observed: S83, S132, S156, S162, S207, S208, S212, S228, and S270. The spectra were reduced using IRAF by following the standard procedure for 2D spectroscopic observations and eighteen 1D spectra were traced and extracted over the sample.

To realise a more extensive study, the sample was increased with H II regions from previous works. We selected from literature those H II regions located at $R_G > 11$ kpc observed in the optical range and with measurements of the electron temperature sensitive lines or, at least, with information about the [S III]λ9068 line. As a result of this search, we found fourteen H II regions that satisfy the stipulated requirements: S98, S127, S128, S158, S203, S206, S209, S219, S255, S266, S283, S298, S301,and S311.

3 Analysis and results

3.1 Line intensities and reddening correction

For the observed H II regions line fluxes were measured by integrating all the flux in the line between two given limits and over a fitted local continuum. The reddening coefficient c(Hβ) was derived from the observed flux ratios of the brightest Balmer lines and all the measured lines were reddening corrected.

For the H II regions selected from the literature, we calculated the original reddened fluxes considering the conditions used by each author and later we re-derived the intensities following the same self-consistent method as in our regions.

The final data set to be analysed consists of 23 H II regions with intensities derived exactly under the same conditions. Hereafter we work with all of these objects as a single sample following the same methodology for both samples.

3.2 Direct chemical abundances

To estimate the chemical abundances, electron density (n_e) and electron temperature (t_e) were required. To obtain the physical conditions of the gas, we performed an iterative process for each region until an agreement was achieved between both parameters. Electron density was calculated from the [S II]$\lambda\lambda$6717,6731 line ratio while electron temperatures were derived using the appropriate line ratios $R_{N2}, R_{O3}, R_{S3}, R_{O2}$, and R'_{S2}.

The ionic chemical abundances were estimated from the forbidden-to-hydrogen emission line ratios of the strongest available emission lines. We derived each ionic abundance with its corresponding electron temperature. The total abundances were also derived, taking into

account, when required, the unseen ionisation stages of each element, using the appropriate ionisation correction factor for each species.

3.3 Tailor-made photoionisation models

For those regions without a detection of any auroral temperature-sensitive emission line we performed tailor-made photoionisation models covering the observed properties of these objects using the code Cloudy v13.03. The models for each region are repeated in an iterative process varying several parameters that most closely reproduces the observed emission lines. The properties obtained from the resulting models are L(Hβ), external radius, oxygen abundance, and N/O ratio. Models were also performed in regions with abundances estimated with the direct method, finding that the two treatments are consistent.

3.4 Relation between radio and optical electron temperatures

Since there is a large sample of nebulae with estimations of electron temperatures based on radio recombination lines and continuum data, we perform a comparative analysis of the optical (t_e) and radio (t_e^*) electron temperatures to derive a relation between them. Radio temperatures derived by [1] and [7] were compared with our optical electron temperatures for H II regions in common to obtain the relation $t_e([O\,III]) = (0.175 \pm 0.080) + (0.792 \pm 0.081) \times t_e^*$. This relation was applied to those regions of the sample without direct estimations of optical temperatures, but with information of t_e^*, to calculate chemical abundances. For two regions, chemical abundances were also derived from photoionisation models; both derivations agree within errors.

4 Discussion

The study of abundance gradients in galaxies is strongly affected by the uncertainty in galactocentric distance: it can affect the slope and, therefore, the interpretation of the results. In order to generate a self-consistent sample, we searched in the literature for the most accurate distances for our sample and we adopted the Galactocentric distances from [2] and [7]. Both groups of authors use the same method (kinematical distances) and they complement each other well since they give distances for different regions or similar estimations for those regions listed in both works.

To derive the radial gradients of metallicity we performed weighted least-squares fits to the distribution of the derived abundances along the Galactocentric distances. Data from the three methods were combined into a single fit. We also computed gradients using only abundances derived for the H II regions with direct determinations of T_e. The final abundance gradients are presented in Table 1. We obtain the radial distribution for the O/H, N/H, N/O, S/H, Ar/H, and He/H abundances; however, for simplicity, in this proceeding we only analyse the results obtained for O/H and N/O (see [4] for a detailed analysis).

Table 1: Final derived abundance gradients towards the Galactic anticentre. Linear least-squares fits weighted by abundances errors computed using all the data (three methods) and using only direct abundances are presented separately. Abundances are in units of dex and Galactocentric radius in units of kpc [4].

Data used	Final abundance gradients
	12+log(O/H)
All data	(9.006 ± 0.112) - (0.053 ± 0.009) R_G
Direct	(9.113 ± 0.139) - (0.061± 0.011) R_G
	12+log(N/H)
All data	(8.260 ± 0.258) - (0.080 ± 0.019) R_G
Direct	(8.331 ± 0.274) - (0.085 ± 0.021) R_G
	log(N/O)
All data	- (0.478 ± 0.086) - (0.041 ±0.006) R_G
Direct	- (0.399 ± 0.095) - (0.047 ± 0.007) R_G
	12+log(S/H)
All data	(8.162 ± 0.088) - (0.106 ± 0.006) R_G
Direct	(8.194 ± 0.089) - (0.108 ± 0.006) R_G
	12+log(Ar/H)
All data	(7.178 ± 0.073) - (0.074 ± 0.006) R_G
	He/H
All data	(0.0968 ± 0.0259) - (0.0005 ± 0.0019) R_G
Direct	(0.0982 ± 0.0299) - (0.0007 ± 0.0022) R_G

The radial distribution of the oxygen abundance is presented in Fig. 1 and it clearly shows a decrease with Galactocentric distance. This result supports the Inside-Out formation scheme of the disc. The inner part of the disc always forms first, and the outer part forms progressively later as gas with higher angular momentum settles into the equatorial plane at larger radii, causing the disc to grow outward with time.

As far as the shape of the gradient is concerned, the possibility of variations in the slope towards the outer disc is still widely debated. Several works have found evidence that the radial abundance gradient of some elements may flatten out at the outer part of the Galaxy disc (e.g. [6] and [10]). In order to analyse the radial behaviour of the abundance gradient in the outermost disc, we need to compare our results (obtained towards the anticentre) with literature gradients performed in wider radial ranges including the inner parts of the Galaxy. When doing so, our data suggest a shallower slope. Although this result does not necessarily imply a flattening of the gradient in the outer disc, what is clear is that the simple extrapolation of the inner slope towards the anticentre is not consistent with the observations.

Figure 2 (left panel) shows the behaviour of N/O versus Galactocentric distance for all the studied regions. The fit of the data presents a decreasing slope in N/O with Galactocentric distance, however our N/O gradient seems to be better represented by a step function instead

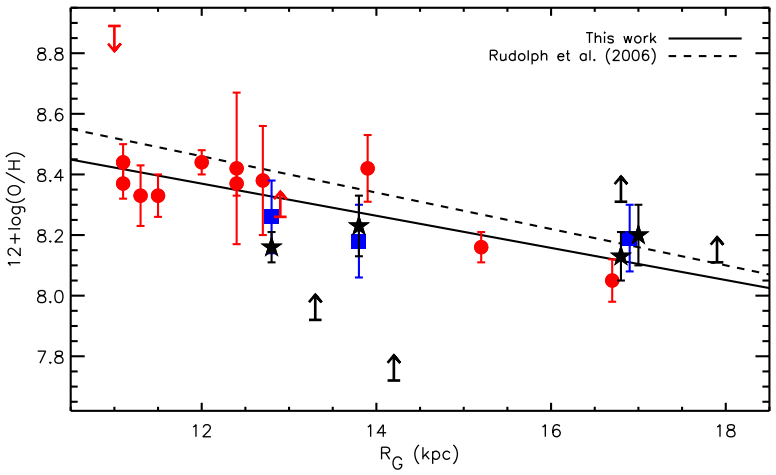

Figure 1: Radial distribution of 12+log(O/H) (in dex) plotted versus Galactocentric radius (R_G in kpc). Red circles denote regions with abundances estimated with direct methods, black squares represent results from tailor-made models, and blue squares plot the abundances obtained from t_e- t_e^* relation. Regions with abundances that are upper or lower limits are represented by arrows. The solid line represents the least-squares weighted fit performed to all the data (except limits abundances), while the extrapolated gradient from [8] is represented by a dashed line. Figure obtained from [4].

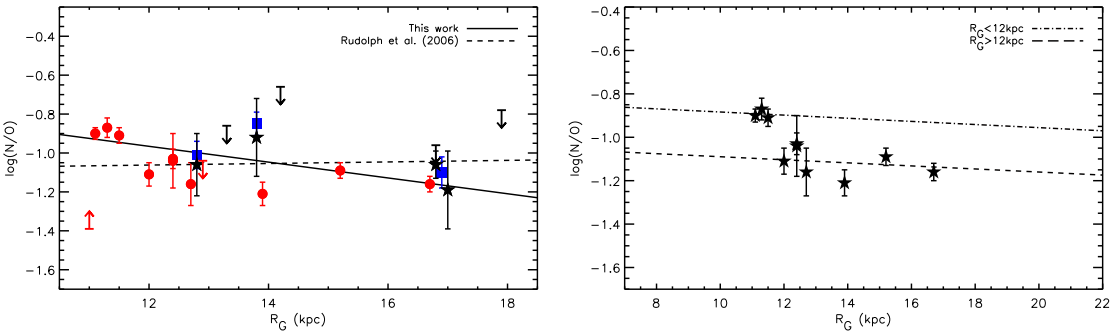

Figure 2: Radial distribution of log(N/O) plotted versus Galactocentric radius. *Left: fit performed using all the data. Symbols and colours are as in Fig. 1. Right: double fit obtained using N/O abundances derived with the direct method. The two lines represent the fit to data in two distances ranges: within 12 kpc from the Galactic centre (dot-dashed line) and farther than this limit (dashed line). Figures obtained from [4].*

of a linear fit. We compute a new double fit using only those N/O abundances derived from the direct method and differentiating those regions placed within 12 kpc from the centre and farther than this limit. The result for R_G <12 kpc is

$\log(N/O) = - (0.7264 \pm 1.3963) + (0.0152 \pm 0.1240)\ R_G$,

while for R_G >12kpc we obtain

$\log(N/O) = - (0.8993 \pm 0.1689) + (0.0150 \pm 0.0116)\ R_G$.

This new double fit is shown in Fig. 2 right panel, and it can be seen that both data sets are represented by lines with similar slopes (nearly constant) but different origins as the N/O ratio is uniform in two distance ranges.

The N/O abundance ratio is a useful indicator of the chemical age of the galaxy and how evolved the disc is. In this case, the fact that N/O is constant informs us that all regions have a similar "chemical age"(understanding age in the sense of the time since the bulk of its star formation occurred). The observed N/O values and radial behaviour in the outer parts of the disc compared to the solar neighbourhood can be understood if we are witnessing a special time in the chemical evolution of the outer MW; in the [3] chemical age scenario this can be a result of the increase in nitrogen abundance from intermediate-mass stars. When comparing our nitrogen distribution with the abundances in the Magellanic Clouds, it can be seen that our N/O ratio appears larger than the value for the SMC and LMC, log(N/O)= -1.58 ± 0.16 and log(N/O)= -1.30 ± 0.30, respectively, for a range in log(O/H) comparable to the abundances measured in the outer disc; this is in line with the chemical ageing scenario mentioned before for the outer disc of the MW.

Acknowledgments

This work has been partially funded by the Spanish projects AYA2013-47742-C4-1, AYA2007-66804, and AYA2012-35330.

References

[1] Balser, D. S., Rood, R. T., Bania, T. M., & Anderson, L. D. 2011, ApJ, 738, 27

[2] Deharveng, L., Peña, M., Caplan, J., & Costero, R. 2000, MNRAS, 311, 329

[3] Edmunds, M. G., & Pagel, B. E. J. 1978, MNRAS, 185, 77P

[4] Fernández-Martín, A., Pérez-Montero, E., Vílchez, J. M., & Mampaso, A. 2016, arXiv:1610.01194

[5] Fich, M., & Blitz, L. 1984, ApJ, 279, 125

[6] Henry, R. B. C., Kwitter, K. B., Jaskot, A. E., et al. 2010, ApJ, 724, 748

[7] Quireza, C., Rood, R. T., Bania, T. M., Balser, D. S., & Maciel, W. J. 2006, ApJ, 653, 1226

[8] Rudolph, A. L., Fich, M., Bell, G. R., et al. 2006, ApJS, 162, 346

[9] Shaver, P. A., McGee, R. X., Newton, L. M., Danks, A. C., & Pottasch, S. R. 1983, MNRAS, 204, 53

[10] Vílchez, J. M., & Esteban, C. 1996, MNRAS, 280, 720